THE JOURNAL OF BIOLOGICAL CHEMISTRY
Vol. 276, No. 22, Issue of June 1, pp. 19396–19403, 2001

Printed in U.S.A.

Structural and Functional Identification of Major Histocompatibility Complex Class I-restricted Self-peptides as Naturally Occurring Molecular Mimics of Viral Antigens

POSSIBLE ROLE IN CD8$^+$ T CELL-MEDIATED, VIRUS-INDUCED AUTOIMMUNE DISEASE*

Received for publication, September 28, 2000, and in revised form, February 7, 2001
Published, JBC Papers in Press, March 8, 2001, DOI 10.1074/jbc.M008864200

Denis Hudrisier‡§¶, Joëlle Riond‡§, Odile Burlet-Schiltz‡§, Matthias G. von Herrath‖, Hanna Lewicki‖, Bernard Monsarrat‡, Michael B. A. Oldstone‖, and Jean Edouard Gairin‡**

From the ‡Institut de Pharmacologie et de Biologie Structurale, CNRS, 205 route de Narbonne, 31400 Toulouse, France and the ‖Department of Neuropharmacology, Division of Virology, Scripps Research Institute, La Jolla, California 92037

Structural similarity (molecular mimicry) between viral epitopes and self-peptides can lead to the induction of autoaggressive CD4$^+$ as well as CD8$^+$ T cell responses. Based on the flexibility of T cell receptor/antigen/major histocompatibility complex recognition, it has been proposed that a self-peptide could replace a viral epitope for T cell recognition and therefore participate in pathophysiological processes in which T cells are involved. To address this issue, we used, as a molecular model of viral antigen, the H-2D^b-restricted immunodominant epitope nucleoprotein (NP)-(396–404) (FQPQNGQFI) of lymphocytic choriomeningitis virus (LCMV). We identified peptide sequences from murine self-proteins that share structural and functional homology with LCMV NP-(396–404) and that bound to H-2D^b with high affinity. One of these self-peptides, derived from tumor necrosis factor receptor I (FGPSNWHFM, amino acids 302–310), maintained LCMV-specific CD8$^+$ T cells in an active state as observed both *in vitro* in cytotoxic assays and *in vivo* in a model of virus-induced autoimmune diabetes, the rat insulin promoter-LCMV NP transgenic mouse. The natural occurrence and molecular concentration at the surface of H-2^b spleen cells of tumor necrosis factor receptor I-(302–310) were determined by on-line μ-high pressure liquid chromatography/mass spectrometry and supported its biological relevance.

Molecular mimicry, a process in which potentially autoreactive T cells are activated in the periphery by major histocompatibility complex (MHC)[1]-restricted cross-reactive self-peptides, is suspected to be a possible mechanism triggering pathological (*versus* normal) immunity, particularly virus-induced autoimmune disease (1). Although the recognition of a viral antigenic peptide by the T cell receptor (TCR) is a most specific process, structurally altered antigenic variants or mimicry peptides, which can be unrelated in terms of primary sequence to the viral antigen (2–4), can still be recognized by CD4$^+$ or CD8$^+$ T cells (5, 6). The functional properties of these peptides depend on their structure, and their interaction with the TCR can lead to either full or partial T cell activation or antagonism (5). Such cross-reactive peptides are thought to play a role in pathophysiological situations such as T cell selection (7, 8), anergy (9), viral escape (10, 11), and autoimmune disorders (12).

Although the development of autoimmune disease has been commonly associated with CD4-bearing T cells (4), there are now both clinical and experimental observations that strongly suggest that autoreactive CD8$^+$ T cells may also be involved (13, 14). However, the molecular mechanisms by which autoreactive CD8$^+$ T cells are activated or maintained in a functional state remain mostly unknown. In this study, we explored the possible role of MHC class I-restricted self-peptides in these mechanisms because of their potential importance in clinical disease. Our aim was (i) to identify putative self-molecular mimics of a viral antigen, (ii) to characterize their structural and functional properties, and (iii) to determine their biological relevance. For this, we used the H-2D^b-restricted immunodominant epitope located in nucleoprotein (NP)-(396–404) (FQPQNGQFI) of lymphocytic choriomeningitis virus (LCMV), a model of choice for dissecting the molecular or cellular mechanisms involved in an autoreactive CD8$^+$ T cell response. Indeed, the H-2D^b-restricted CD8$^+$ T cell response mounted against the LCMV NP is directed toward the immunodominant epitope sequence NP-(396–404) (15–17). The LCMV-infected mouse typically undergoes activation and massive expansion of CD8$^+$ T cells, which consistently stay at a high level throughout the animal's life span, even in the absence of detectable virus and/or viral antigen (18–20). These cytotoxic T cells (CTLs) represent a potential source of autoreactivity, particularly if their cytolytic function remains intact. The H-2^b transgenic mice, which express LCMV NP under the control of the rat insulin promoter (RIP), represent an *in vivo* model of autoimmune disease (21, 22) in which LCMV NP-(396–404) can be the target of autoreactive CTLs. After LCMV infection or adop-

* This work was supported in part by grants from CNRS; Association pour la Recherche sur le Cancer Contract 5485, Région Midi-Pyrénées; National Institutes of Health Grants AI41439, AI09484 (to M. B. A. O.), and AI44451 (to M. G. v. H.); and a Juvenile Diabetes International Foundation career development award (to M. G. v. H.). This is Publication 13360-NP from the Department of Neuropharmacology, Scripps Research Institute (La Jolla, CA). The costs of publication of this article were defrayed in part by the payment of page charges. This article must therefore be hereby marked "*advertisement*" in accordance with 18 U.S.C. Section 1734 solely to indicate this fact.

§ These authors contributed equally to this work.

¶ Present address: INSERM U395, CHU Purpan, 31059 Toulouse Cedex, France.

** To whom correspondence should be addressed. Tel.: 33-561-175-530; Fax: 33-561-175-532; E-mail: gairin@ipbs.fr.

[1] The abbreviations used are: MHC, major histocompatibility complex; TCR, T cell receptor; NP, nucleoprotein; LCMV, lymphocytic choriomeningitis virus; CTL, cytotoxic T lymphocyte; RIP, rat insulin promoter; IDDM, insulin-dependent diabetes mellitus; TNFR, tumor necrosis factor receptor; HPLC, high pressure liquid chromatography; ESI-MS, electrospray ionization mass spectrometry; IFN-γ, interferon-γ.

tive transfer of anti-LCMV CTLs, these RIP-LCMV NP mice develop insulin-dependent diabetes mellitus (IDDM), a virus-induced autoimmune disease in which both $CD4^+$ and $CD8^+$ T cells are involved (23). In these mice, the destruction of β cells and ensuing IDDM have been attributed to MHC class I-restricted $CD8^+$ T cells (22, 24, 25). Furthermore, the finding that IDDM does not develop in MHC class I-deficient mice or CD8-depleted mice (24) provides additional support for the involvement of $CD8^+$ T cells and, consequently, of MHC class I-restricted self-peptides.

Here, we first identified a set of six nonameric sequences from endogenous proteins sharing structural and functional homology with LCMV NP-(396–404). Five of these endogenous peptides bound with high affinity to H-$2D^b$ and generally acted as antagonists of lysis by LCMV-specific CTLs. In the presence of H-2^b cells pulsed with three of these peptides, LCMV-specific CTLs were maintained in long-term culture. We then selected one of these peptides, tumor necrosis factor receptor I (TNFR)-(302–310), which activated LCMV NP-specific CTLs, allowing them to kill LCMV-infected cells in a peptide-specific, MHC-restricted manner. Adoptive transfer of TNFR-(302–310)-activated CTLs into RIP-LCMV NP $\times$ RIP-B7.1 transgenic mice provoked a specific destruction of β cells of the islets of Langerhans and caused IDDM. Using on-line μ-high pressure liquid chromatography (HPLC)/electrospray ionization mass spectrometry (ESI-MS), we demonstrated the presence of TNFR-(302–310) at the surface of H-2^b spleen cells, a finding supporting its biological relevance.

EXPERIMENTAL PROCEDURES

Cell Lines, Mice, and CTLs—The T2 human mutant cell line transfected with H-$2D^b$ (T2-D^b) (26) was used in binding experiments. The murine H-2^b cell lines MC57 and RMA and the H-2^d cell line BALB/cl7 were used as target cells in CTL assays. Cells were grown in RPMI 1640 medium (MC57, RMA, and BALB/cl7) or Iscove's modified Dulbecco's medium (T2-D^b) containing 8% bovine serum, L-glutamine, and antibiotics. Geneticin (400 μg/ml) was added to Iscove's modified Dulbecco's medium to maintain selection of positively transfected T2-D^b cells. C57BL/6 (H-2^b) and BALB/c (H-2^d) mice were obtained from the breeding colony at the Scripps Research Institute. CTL clone NP18, specific for the H-$2D^b$-restricted LCMV epitope NP-(396–404) (27), was restimulated weekly with LCMV-infected MC57 cells and spleen cells from C57BL/6 mice. Polyclonal CTLs were generated by cultivating naive spleen cells from C57BL/6 mice with 1 μM LCMV NP-(396–404) without interleukin-2 for 10 days and then restimulated weekly using LCMV NP-(396–404)-coated RMA cells and spleen cells from C57BL/6 mice in the presence of interleukin-2 (30 units/ml). CTLs used in long-term culture studies or adoptive transfer experiments were generated from C57BL/6 and control BALB/c mice infected with 10^5 plaque-forming units of the LCMV Arm strain intraperitoneally. 45–60 days later, a single suspension of spleen cells was cultured with or without peptide-pulsed (1 μg/ml) or LCMV-infected macrophages.

MHC Binding Studies—Peptide binding to H-$2D^b$ was determined in a competition assay as previously described (28). T2-D^b cells (1×10^5 cells/well) were incubated with fluorescein isothiocyanate-labeled KAIENAEAL (100 nM) for 75 min at 37 °C in the presence of proteases inhibitors. Total binding and nonspecific binding were measured in the absence or presence of 1 mM unlabeled peptide, respectively. Cells were washed with 1% bovine serum albumin in phosphate-buffered saline and fixed in 1% paraformaldehyde, and the fluorescence (mean fluorescence intensity (mfi)) was analyzed by fluorescence-activated cell sorting (Becton-Dickinson). Assays were performed with increasing concentrations (10^{-10} to 10^{-5} M) of unlabeled competitors. Specific binding to H-$2D^b$ was defined as the difference between total and nonspecific binding. The percentage inhibition of binding was calculated as $100 \times (1 - (\text{mfi in presence of competitor} - (\text{mfi(nonspecific binding)}/\text{mfi(specific binding)})))$. The 50% inhibiting concentration (IC_{50}) corresponds to a peptide concentration inhibiting half the maximal specific binding of fluorescein isothiocyanate-labeled KAIENAEAL to H-$2D^b$.

Peptide Search in Data Bases—An algorithm was used to search for murine nonameric peptides sharing functional homology with LCMV NP-(396–404) in the Swiss Protein Database. Criteria (illustrated in Fig. 1) were as follows: at P1, all 20 amino acids except Leu, Ile, Met, and Val; at P2, Ala, Asn, Cys, Gln, Gly, and Ser; at P3, Leu, Met, Ile, Val, Pro, and Ala; at P4, all amino acids; at P5, Asn; at P6, all amino acids; at P7, all amino acids; at P8, Phe; and at P9, Leu, Ile, and Met. Restrictions at P1, P2, P3, P5, and P9 were imposed according to published studies (29–31).

In Vitro Cytotoxic Assays—LCMV-infected or peptide-pulsed uninfected target cells were incubated for 1 h at 37 °C with ^{51}Cr and washed, and LCMV-specific CTLs were added at the indicated effector/target ratio. Target and effector cells were incubated at 37 °C in a final volume of 200 μl. After a 5-h incubation period, fractions (100 μl) were removed and counted for ^{51}Cr activity. The percent specific lysis was calculated as $100 \times ((\text{cpm(experimental release)} - \text{cpm(spontaneous release)})/(\text{cpm(total release)} - \text{cpm(spontaneous release)}))$. Total release and spontaneous release were determined by incubating the labeled cells with 1% Nonidet P-40 and culture medium, respectively. In all experiments, samples were run in triplicate, and the mean values are given. Antagonism was assayed in a 5-h ^{51}Cr release assay as described above, except that RMA cells were prepulsed with a suboptimal concentration of LCMV NP-(396–404) (giving 30–40% lysis) during ^{51}Cr labeling, extensively washed, and incubated with a 1, 10, or 100 μM concentration of the indicated peptides for 30 min at 37 °C before CTLs were added at an effector/target ratio of 5:1.

IFN-γ Production—RMA cells (3×10^3 cells/well) were incubated for 1 h at 37 °C in the presence of the indicated peptides (1×10^{-10} to 1×10^{-5} M). CTLs (15×10^3 cells/well) were then added and incubated with target cells for 24 h at 37 °C. The IFN-γ present in the supernatant was measured by enzyme-linked immunosorbent assay using R4-6A2 and biotinylated XMG1.2 as the pair of antibodies (a kind gift of Dr. J.-C. Guery). Horseradish peroxidase-conjugated streptavidin (Amersham Pharmacia Biotech) was used to detect biotinylated XMG1.2, followed by incubation with *o*-phenylenediamine hydrochloride (Sigma). The color was red at 490 nm using an enzyme-linked immunosorbent assay reader (Titertek Multiskan Plus MKII, EFLAB, Finland) and normalized to the values obtained for a standard curve of recombinant murine IFN-γ (Sigma).

Proliferation Assay—CTLs (1×10^4) were mixed with RMA cells (5×10^4) previously γ-irradiated (10,000 rads) and pulsed with peptide (1 μM). Cells were incubated for 72 h at 37 °C and with 1 μCi of [^{3}H]thymidine during the last 16 h. The level of [^{3}H]thymidine incorporation was then determined by scintillation counting.

Adoptive Transfer and in Vivo Immunopathology Assay—H-2^b or H-2^d double RIP-LCMV NP $\times$ RIP-B7.1 transgenic mice expressing LCMV NP $\times$ B7.1 in β cells of islets of Langerhans were adoptively transferred with 2×10^7 long-term cultured T cells maintained as described above and inoculated intraperitoneally. Blood glucose levels were monitored, and pancreatic tissues were studied by immunohistochemistry for evidence of CTL infiltration as previously described (22, 24, 40).

Extraction of Endogenously Presented Peptides from Spleen Cells—Peptides were acid-extracted from the cell surface as previously described (32). Briefly, splenocytes ($1–2 \times 10^9$ cells) were washed three times with phosphate-buffered saline and then resuspended in 0.131 M citric acid and 0.066 M Na_2HPO_4 at pH 3.0 for 2 min. The eluted material was desalted on Waters Sep-Pak column according to the manufacturer's instructions, vacuum-concentrated, and centrifuged in 1% trifluoroacetic acid on a Centricon 3 (3-kDa cutoff; Amicon, Inc.) at $3800 \times g$ for 90 min at 4 °C. The filtered material was vacuum-concentrated and resuspended in 100 μl of 0.08% trifluoroacetic acid. Peptides were separated on a reversed-phase C_{18} column (Aquapore, 7 μm, 2.1 $\times$ 100 mm; Brownlee) using a Waters 600S controller system. Samples (25 μl) were injected and separated using a system gradient of 5–36% solvent B for a 60-min period at a flow rate of 200 μl/min. Solvent A was 0.08% trifluoroacetic acid in H_2O, and solvent B was 0.08% trifluoroacetic acid in CH_3CN. Fractions (200 μl) were collected, lyophilized, and stored at −80 °C until analysis by on-line μ-HPLC/ESI-MS.

Structural Identification of Naturally Occurring Peptides by On-line μ-HPLC/ESI-MS—The collected HPLC fractions were injected on a reversed-phase C_{18} microcolumn (PepMap™, 3 μm, 0.3 $\times$ 150 mm; LC Packings). Elution was performed with a gradient of 5–55% solvent B in 25 min. Solvent A was 0.05% acetic acid in 95:5 (v/v) H_2O/CH_3CN, and solvent B was 0.05% acetic acid in 20:80 (v/v) H_2O/CH_3CN. The flow rate was set at 400 μl/min and split to 4 μl/min before the column. MS data were recorded on a Finnigan MAT TSQ700 triple quadrupole mass spectrometer equipped with an electrospray source either by scanning the range of masses corresponding to m/z values between 300 and 1800 every 3 s or by using the "single ion monitoring" mode, where the quadrupole is set to transmit only one particular m/z value, corresponding to an ion of interest, centered in a 1-m/z unit window. Low

TABLE I

H-2D^b binding and CTL recognition of the LCMV NP-(396–404) epitope and monoalanine-substituted analogs

Peptides were synthesized by the solid-phase method using Fmoc (*N*-(9-fluorenyl)methoxycarbonyl) chemistry and purified by HPLC on a reversed-phase RP300 C_8 column (Brownlee), and their identities were confirmed by ESI-MS analysis. For H-2D^b binding experiments, peptides (10^{-10} to 10^{-5} M) were tested in a MHC class I competition assay on T2-D^b cells as described previously (28). IC_{50} values represent the peptide concentrations inhibiting half the maximal binding of the labeled peptide. Values are the means ± S.E. of three independent experiments. For CTL recognition, peptides (10^{-12} to 10^{-6} M) were tested in a classical CTL assay by measuring the lysis of peptide-coated MC57 target cells by NP-specific CTL clone NP18 (effector/target ratio of 5:1). EC_{50} values represent the peptide concentrations inducing half of the maximal lysis effect. Values from one experiment are shown and are representative of several independent experiments. Residues implicated in either MHC binding or TCR recognition are shown in boldface italic type.

Peptide									IC_{50} for H-2D^b binding	EC_{50} for CTL recognition
1	2	3	4	5	6	7	8	9		
									nM	*nM*
Phe	Gln	Pro	Gln	Asn	Gly	Gln	Phe	Ile	13 ± 1	0.008
Ala	Gln	Pro	Gln	Asn	Gly	Gln	Phe	Ile	14 ± 2	***>1000***[a]
Phe	**Ala**	Pro	Gln	Asn	Gly	Gln	Phe	Ile	5 ± 1	0.03
Phe	Gln	**Ala**	Gln	Asn	Gly	Gln	Phe	Ile	***95 ± 17***	**1000**
Phe	Gln	Pro	**Ala**	Asn	Gly	Gln	Phe	Ile	9 ± 1	***8***
Phe	Gln	Pro	Gln	**Ala**	Gly	Gln	Phe	Ile	***114 ± 19***	**8**
Phe	Gln	Pro	Gln	Asn	**Ala**	Gln	Phe	Ile	14 ± 3	0.09
Phe	Gln	Pro	Gln	Asn	Gly	**Ala**	Phe	Ile	13 ± 2	0.04
Phe	Gln	Pro	Gln	Asn	Gly	Gln	**Ala**	Ile	19 ± 1	***No lysis***[b]
Phe	Gln	Pro	Gln	Asn	Gly	Gln	Phe	**Ala**	***37 ± 6***	**0.1**

[a] 15% specific lysis was observed at the highest peptide concentration tested (10^{-6} M).
[b] No specific lysis (<5%) occurred even at the highest peptide concentration tested (10^{-6} M).

energy collision-activated dissociation MS/MS experiments were conducted in the "selected reaction monitoring" mode, where the first quadrupole is set to transmit the precursor ion of interest and the third quadrupole is scanned over a 10-m/z unit mass range centered on the m/z value of the fragment ion of interest. Argon was used as the collision gas at a collision pressure of 1.2 millitorr. The collision energy was 28 eV in the laboratory frame of reference.

Molecular Modeling of H-2D^b/Peptide Interactions—The H2-D^b structure was obtained from crystallographic data of H-2D^b with influenza virus peptide NP-(366–374) (33). The LCMV NP-(396–404) and TNFR-(302–310) nonamers were introduced manually using the program O. Side chain conformation was based on the most probable rotamer and the probable hydrogen bonds. After transfer of H-2D^b data to Insight II (Biosym Technologies), minimization was done using the VA09A (1000 iterations without constraints) algorithm.

RESULTS

Structural and Functional Anatomy of the LCMV NP-(396–404) Epitope—We first identified the residues of LCMV NP-(396–404) involved in MHC binding and those serving as TCR contacts. Binding assays of monoalanine-substituted analogs (Table I) confirmed Asn^{400} at P5 and Ile^{404} at the C terminus as H-2D^b anchors. Pro^{398} at P3 contributed significantly to MHC binding, likely by pointing down to the MHC-binding groove (33) and/or, as a proline residue, by inducing structural constraints to the peptide backbone (34). The impact of alanine substitution on the ability of NP-(396–404) to sensitize target cells to lysis by LCMV-specific CTLs was then assessed. Results obtained with the NP-(396–404)-specific CTL clone NP18 (35) are shown in Table I. The strongest effect was observed at position 8, where substitution of Ala for Phe yielded a peptide totally unable to sensitize target cells even at the highest concentration tested, indicating that Phe^{403} is the critical (main) TCR contact. CTL sensitization properties were also profoundly altered, but not abolished, after substitution of Phe^{396} at P1 and Gln^{399} at P4, indicating that these two residues also play a role, although of lesser importance, as TCR (auxiliary) contacts. Substitution of residues at positions 2 (Gln), 6 (Gly), 7 (Gln), and 9 (Phe) had little effect. The effects observed at positions 3 and 5 were expected as a consequence of the weak MHC-binding properties of the analogs. Similar results were obtained with polyclonal populations of CTLs obtained from C57BL/6 mice either infected with LCMV Arm or immunized with synthetic NP-(396–404) (data not shown). These three main (Phe^{403}) and auxiliary (Phe^{396} and Gln^{399}) TCR contacts identified in the NP-(396–404) sequence undoubtedly represent the overall CTL response against this antigen. A summary of MHC binding and TCR interactions is illustrated in Fig. 1*A*.

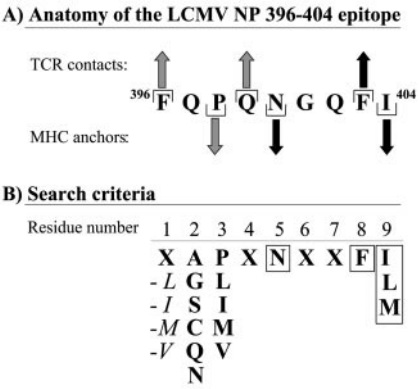

FIG. 1. **Screening strategy for murine self-peptides that have minimal functional homology to LCMV NP-(396–404).** *A*, anatomy of the viral epitope. Residues implicated in MHC binding or in TCR interactions were identified using the monoalanine scanning approach. The main and auxiliary interactions are shown as *black* and *stippled arrows*, respectively. *B*, search criteria for nonameric self-peptide sequences sharing minimal functional homology with LCMV NP-(396–404) (FQPQNGQFI). We searched the Swiss Protein Database by (i) fixing the required functional amino acids at P5, P8, and P9; (ii) imposing or excluding some amino acids known to play a positive (at P2 and P3) or negative (at P1) role in H-2D^b binding (31); and (iii) allowing any of the 20 natural amino acids at P4, P6, and P7.

Search for Murine Self-peptides Sharing Minimal Functional Homology with LCMV NP-(396–404)—We next screened the Swiss Protein Database for murine nonameric self-peptides fulfilling the following requirements (Fig. 1*B*). The two H-2D^b anchors must be present at P5 (Asn) and P9 (Met, Leu, or Ile) (29) as well as the main CTL contact at P8 (Phe) of NP-(396–404). Additional criteria were imposed at P1, P2, and P3, for which some residues affect peptide presentation by H-2D^b (30, 31). Finally, no restriction was applied to P4, P6, and P7, at which structural modification has no or little impact on NP binding. About 30 peptides were extracted from the registered murine proteins, with a high proportion of redundant sequences (*i.e.* different members of the same protein family registered under different code numbers). From them, we selected the only six sequences from non-redundant proteins

TABLE II

Self-peptides from murine proteins with minimal functional homology to LCMV NP-(396–404)

Murine nonameric peptides with functional homology to LCMV NP-(396–404) were extracted from the Swiss Protein Database according to the search criteria illustrated in Fig. 1*B*. For a given position, homologous residues are shown in boldface. Peptide binding to H-2D^b was determined as described in the legend to Table I. Values are the means ± S.E. of three independent experiments.

Peptide	Sequence	Homology	Origin of protein	Cellular location	Tissue distribution	IC_{50} for H-2D^b affinity
						nM
NP-(396–404)	**F**Q**P**Q**N**G**Q**F**I**	—	Viral nucleoprotein	Cytosol	Infected cells, broad	5.7 ± 1.4
TNFR-(302–310)	**F**G**P**S**N**W**H**F**M**	5/9 (56%)	TNFR-I	Membrane	Tumor, lymphoid cells	0.65 ± 0.34
LAP-(177–185)	RSI**Q**NA**Q**F**L**	5/9 (56%)	Lysosomal acid phosphatase	Lysosome	Ubiquitous	8.7 ± 1.8
PKC-(351–359)	**F**GID**N**FE**F**I	4/9 (44%)	Protein kinase Cλ	Cytosol, membrane	Skin, lung	0.12 ± 0.04
IgVH-(91–99)	DN**P**K**N**TL**F**L	4/9 (44%)	Ig heavy chain, V region	Cytosol	β cells, extracellular fluids	1200 ± 208
NCad-(569–577)	NNIY**N**AT**F**L	3/9 (33%)	N-cadherin	Membrane	Neurons	29.3 ± 1.3
LDH-(282–290)	YGIE**N**EV**F**L	3/9 (33%)	Lactate dehydrogenase, heavy chain	Cytosol	Heart muscle	1.5 ± 0.2

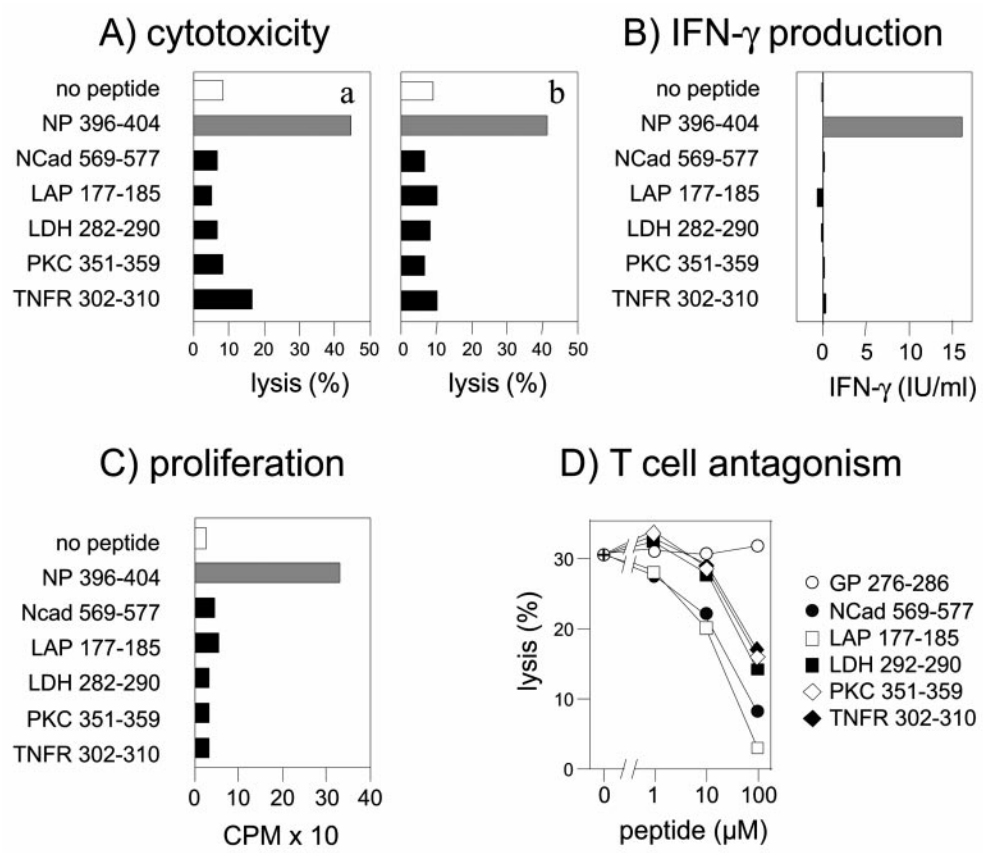

FIG. 2. **Functional properties of murine self-peptides upon reacting with H-2D^b class I-restricted LCMV NP-(396–404)-specific CTLs.** *A*, sensitization of target cells to lysis by CTL clone NP18 (*panel a*) or polyclonal CTLs (*panel b*) specific for LCMV NP-(396–404) was analyzed in a ^{51}Cr release assay as described under "Experimental Procedures." *B*, IFN-γ production. Enzyme-linked immunosorbent assays were carried out as described for the cytotoxicity assays, except that supernatants were collected after 24 h and tested for IFN-γ content. Results are expressed as international units/ml and are representative of two independent experiments. *C*, proliferation. T cells (1×10^4) were mixed with γ-irradiated, peptide-pulsed RMA cells (5×10^4) and incubated for 72 h at 37 °C. [^{3}H]Thymidine was added during the last 16 h, and incorporation was determined by scintillation counting. *D*, T cell antagonism. The antagonist properties of the self-peptides were assessed in cytotoxicity assays. RMA cells were loaded with a suboptimal concentration (giving <50% maximal lysis) of LCMV NP-(396–404); washed; and incubated with a 1, 10, or 100 μM concentration of the indicated peptide before addition of CTLs. Results are from one representative experiment among three. *NCad*, N-cadherin; *LAP*, lysosomal acid phosphatase; *LDH*, lactate dehydrogenase; *PKC*, protein kinase Cλ; *GP*, glycoprotein.

(Table II). In addition to the two main MHC anchors and the main TCR contact (minimal functional homology), some of these peptides presented a higher sequence homology by sharing one or two other residues with LCMV NP-(396–404). The six murine self-peptides (mimicry peptides) were then tested for binding to H-2D^b. As shown in Table II, five of them bound efficiently to H-2D^b with affinities comparable to (lysosomal acid phosphatase-(177–185) and lactate dehydrogenase-(282–290)), higher than (protein kinase C-(351–359) and TNFR-(302–310)), or lower than (N-cadherin-(569–577)) that of NP-(396–404). Only one peptide, IgVH-(91–99) (Ig V region heavy chain), was a weak H-2D^b binder and, for this reason, was not studied further.

Recognition of the Murine Self-peptides by LCMV NP-(396–404)-specific CTLs—The capacity of the five mimicry peptides to activate such functions of LCMV NP-specific CTLs as cytotoxicity, IFN-γ production, proliferation, and Ca^{2+} mobilization was then evaluated. As shown in Fig. 2*A*, no significant lysis of target cells was observed in the presence of the self-peptides. LCMV NP-(396–404) induced a strong IFN-γ production (Fig.

TABLE III
Fate of LCMV-specific H-2^b CTLs as culture conditions vary

C57BL/6 mice were infected with LCMV Arm (1×10^5 plaque-forming units intraperitoneally). 45–60 days after infection, a single suspension of splenic lymphoid cells (10^6 cells/ml) containing LCMV-specific CTLs was cultured in the presence of irradiated bulk naive splenocytes (5×10^6) from C57BL/6 mice and irradiated H-2^b macrophages as antigen-presenting cells (APCs) infected with LCMV Arm (I), coated with the H-2D^b-restricted (NP-(396–404)) or H-2L^d-restricted (NP-(118–126)) LCMV epitopes (II), coated with the self-peptide (III), or untreated (IV). NCad, N-cadherin; PKC, protein kinase Cλ.

	Culture conditions	Fate of LCMV-specific CTLs
I.	APCs infected with LCMV Arm	Long-term growth and maintenance, **>2 months**
II.	APCs coated with LCMV NP-(396–404)	Long-term growth and maintenance, **>2 months**
	APCs coated with LCMV NP-(118–126)	Short-term growth and death, >10 days
III.	APCs coated with NCad-(569–577)	Long-term growth and maintenance, **>2 months**
	APCs coated with PKC-(351–359)	Long-term growth and maintenance, **>2 months**
	APCs coated with TNFR-(302–310)	Long-term growth and maintenance, **>2 months**
IV.	APCs (untreated)	Short-term growth and death, <10 days

2*B*) and T cell proliferation (Fig. 2C), as expected. In contrast, none of the self-peptides incited either IFN-γ production or measurable T cell proliferation *in vitro*. Similar results were obtained when Ca^{2+} mobilization was analyzed (data not shown).

The Murine Self-peptides Homologous to LCMV NP-(396–404) Are Antagonists of the NP-specific TCR—Since structural modification can alter TCR recognition by provoking partial agonism or antagonism (36–39), we next determined if the self-peptides could behave as antagonists. Fig. 2*D* depicts the reduced lytic function of the NP-specific CTLs by the murine self-peptides with minimal homology to NP-(396–404). Lysis of labeled target cells coated with suboptimal concentrations of NP-(396–404) was inhibited in the presence of increasing concentrations of synthetic self-peptides, *i.e.* 50–90% inhibition was reached at the highest concentration tested (100 μM). In negative control experiments, no antagonism was detected with the two other H-2D^b-restricted LCMV immunodominant epitopes: glycoprotein-(276–286), which binds to H-2D^b with a high affinity, similar to that of NP-(396–404) (15) (Fig. 2), and glycoprotein-(33–41) (data not shown).

Long-term Maintenance of LCMV-specific CTLs by Mimicry Peptides—To determine whether mimicry peptides could maintain anti-LCMV CTLs in long-term culture, we used single suspensions of spleen cells from C57BL/6 mice 45–60 days after LCMV infection. Such splenocytes contain numerous anti-LCMV and particularly anti-NP-(396–404) memory CTLs (17). These CTLs were cultured with macrophages coated with peptide, infected with LCMV, or left untreated. The three peptides selected for this study, N-cadherin-(569–577), protein kinase C-(351–359), and TNFR-(302–310), shared three, four, and five functional residues with LCMV NP-(396–404), respectively (see Table II). As summarized in Table III, in the absence of stimulatory signals, T cells died in culture within 2 weeks, whereas stimulation by cells infected with LCMV or pulsed with the synthetic LCMV NP-(396–404) peptide routinely resulted in a long-term maintenance of anti-LCMV CTLs. The three mimicry peptides tested allowed the anti-LCMV CTLs to grow in culture in the long-term range. In contrast, CTLs died within 2 weeks when cultured in the presence of unmatched MHC (H-2^d) macrophages pulsed with the H-2L^d-restricted LCMV NP-(118–126) immunodominant epitope.

In Vitro and in Vivo Activities of Long-term Cultured CTLs Stimulated with TNFR-(302–310)—We next determined whether antiviral CTLs maintained in long-term culture in the presence of a mimicry peptide retained functional MHC-restricted activity. We used the self-peptide TNFR-(302–310) for these studies. As presented in Table IV, CTLs stimulated with TNFR-(302–310) lysed LCMV-infected H-2^b targets. However, the efficiency was lower than that observed with CTLs stimulated with LCMV or NP-(396–404). In control experiments, H-2^b targets pulsed with the synthetic NP-(396–404) or TNFR-(302–310) peptide were also lysed by CTLs, whereas H-2^d targets coated with the H-2L^d-restricted epitope NP-(118–126) were not lysed (data not shown).

TABLE IV
In vitro cytotoxic activity of long-term cultured LCMV-specific CTLs

LCMV-specific CTLs obtained from LCMV-infected C57BL/6 mice and cultured with LCMV-infected or peptide-pulsed macrophages as described in the legend to Table III were used. Their capacity to lyse LCMV-infected target cells was tested in a 5-h ^{51}Cr release assay at an effector/target ratio of 2.5:1 as described under "Experimental Procedures." LCMV-specific CTLs had been in culture for 3 months at the time the assay was performed. Results from one experiment are shown and are representative of three independent experiments.

LCMV-infected target cells	Specific lysis of LCMV-specific CTLs cultured with:		
	LCMV	Peptides	
		NP-(396–404)	TNFR-(302–310)
	%		
MC57 (H-2^b)	56	49	29
BALB/cl7 (H-2^d)	1	5	5

We then determined whether the TNFR-(302–310)-stimulated CTLs had preserved cytotoxic activity *in vivo*. For this purpose, such CTLs were adoptively transferred into double RIP-LCMV NP × RIP-B7.1 transgenic mice. In such mice, either LCMV infection or adoptive transfer of anti-NP-(396–404) CTLs causes CTL infiltration into the islets of Langerhans, insulitis, and IDDM as measured by the elevation of blood glucose and reduction of pancreatic insulin (21, 22, 40). As shown in Table V, insulitis and elevated blood glucose levels indicating IDDM were observed in recipients of adoptively transferred LCMV-specific CTLs previously co-cultured with TNFR-(302–310) for >2 months. Immunohistochemical analysis confirmed CTL infiltration into the pancreases of these mice (data not shown). Specificity was demonstrated when H-2^d transgenic mice failed to develop insulitis or IDDM after adoptive transfer of H-2^b-restricted CTLs primed by TNFR-(302–310)-coated or LCMV-infected macrophages.

The TNFR-(302–310) Peptide Is Naturally Presented at the Surface of H-2^b Spleen Cells—The final and important step was to document that such a self-peptide with the ability to maintain functional virus-specific CTLs was present at the cell surface. To do so, peptides were extracted from the surface of splenocytes, separated by HPLC, collected into fractions of interest, and then analyzed by on-line μ-HPLC/ESI-MS. Because the TNFR-(302–310) peptide contained a methionine residue, its chemical modification was expected during the extraction and analysis process. Indeed, as a control, the synthetic TNFR-(302–310) peptide eluted in two distinct peaks, fractions 52 and 58 (Fig. 3, *STEP-1*, *F52* and *F58*). As assessed by MS, fraction 58 corresponded to the unmodified form of the synthetic peptide ($(M + 2H)^{2+}$, m/z 561.9), and fraction 52

TABLE V

In vivo activity of LCMV-specific CTLs after adoptive transfer into H-2^b RIP-LCMV NP × B7.1 transgenic mice

H-2^b or H-2^d transgenic mice expressing LCMV NP × B7.1 in β cells of islets of Langerhans using the RIP were used. Mice were adoptively transferred with 2×10^7 long-term cultured CTLs activated as described in the legend to Table III and inoculated intraperitoneally. Blood glucose (BG) levels were monitored, and CTL infiltration of pancreatic tissues was studied as described (22, 24, 40).

Transfer of LCMV-specific CTLs to:	Mice with infiltration or elevated BG	
	Insulitis	IDDM
H-2^b RIP-LCMV NP × RIP-B7.1		
LCMV-specific CTLs cultured with LCMV	3/3	3/3
LCMV-specific CTLs cultured with TNFR-(302–310)	3/3	3/3 (BG, 412, 312, 482)[a]
H-2^d RIP-LCMV NP × RIP-B7.1		
LCMV-specific CTLs cultured with TNFR-(302–310)	0/3	0/3

[a] CTL infiltration into the pancreases of these mice was observed by immunohistochemistry analysis (data not shown).

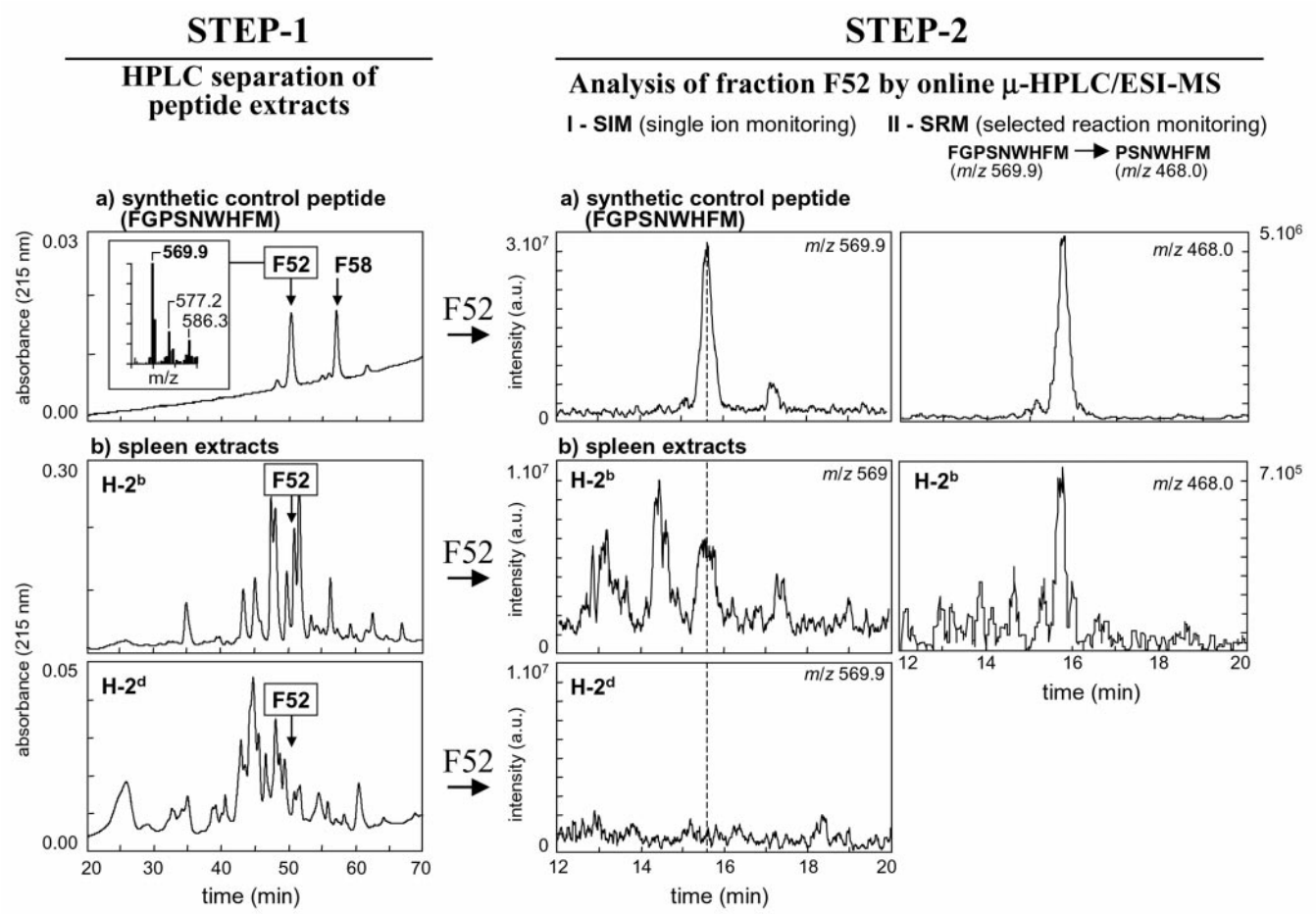

FIG. 3. **On-line μ-HPLC/ESI-MS identifies the naturally occurring self-peptide TNFR-(302–310) on the surfaces of H-2^b spleen cells.** In the first step (*STEP-1*), acid-eluted peptides from C57BL/6 (H-2^b) or Dba/2 (H-2^d) splenocytes or a mock extract of synthetic TNFR-(302–310) were fractionated by HPLC as described under "Experimental Procedures." The oxidized and unmodified forms of TNFR-(302–310) eluted in fractions 52 (*F52*) and 58 (*F58*), respectively. The mass spectrum of fraction 52 is shown in the *inset* in *panel a* (m/z 569.9 corresponds to the $(M + 2H)^{2+}$ ion of the oxidized form). In the second step (*STEP-2*), the respective fractions 52 were collected and further analyzed by on-line μ-HPLC/ESI-MS (*left panels*) using the single ion monitoring detection mode at m/z 569.9. Plots show the ion current from aliquots corresponding to 1×10^8 cells. Low energy collision-activated dissociation MS/MS experiments were conducted in the selected reaction monitoring mode (*right panels*), where the first quadrupole is set to transmit the precursor ion of interest (m/z 569.9), corresponding to FGPSNWHFM, and the third quadrupole is scanned over the 10-m/z unit mass range centered on the m/z value of the fragment ion of interest (m/z 468.0), corresponding to PSNWHFM. *a.u.*, arbitrary units.

corresponded to the chemically modified form bearing an oxidized C-terminal methionine ($(M + 2H)^{2+}$, m/z 569.9; as shown in Fig. 3, *STEP-1*, *panel a*, *inset*). When analyzed at different concentrations (10–1000-fold dilutions), we noted that the susceptibility of TNFR-(302–310) to oxidation both under sample storage conditions and during analysis increased with peptide dilution (data not shown). Peptides extracted from C57BL/6 (H-2^b) and control BALB/cl7 (H-2^d) spleen cells were then separated, and their respective fractions 52 were collected and analyzed by on-line μ-HPLC/ESI-MS (Fig. 3, *STEP-2*). An ion whose mass and retention time were identical to those of the oxidized form of the synthetic TNFR-(302–310) peptide was clearly detected in fraction 52 of H-2^b (but not H-2^d) spleen extracts. Identification of this natural form of TNFR-(302–310) was unambiguously confirmed by (i) overloading experiments, which gave a perfectly superimposable coelution of the natural product and the overloaded synthetic oxidized form; and (ii) MS/MS experiments, which produced a fragment ion specific for the oxidized TNFR-(302–310) peptide upon collision, as detected by selected reaction monitoring (Fig. 3, *STEP-2*, *right*

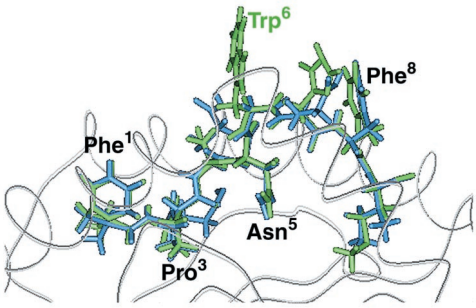

FIG. 4. **Side view of the superimposed structures of LCMV NP-(396–404) and TNFR-(302–310) in the H-2D^b-binding groove.** The α_1- and α_2-MHC domains are shown as *gray ribbons*. The peptides are shown as *blue* (LCMV NP-(396–404), FQPQNGQFI) or *green* (TNFR-(302–310), FGPSNWHFM) *sticks*. The model shows the perfect superimposition of the two peptide backbones and of the side chains of the shared residues Phe^1, Pro^3, Asn^5, and Phe^8. The model also illustrates the steric hindrance of the bulky side chain of Trp^6 of TNFR-(302–310), which points out of H2-D^b and likely results in altered TCR/peptide/MHC interactions.

panels). Based on the measured ionic current intensity, the amount of the TNFR-(302–310) peptide extracted from 10^8 H-2^b spleen cells was ~120 fmol. Given the yield of the extraction procedure (10–15%), the amount of TNFR-(302–310) detected on the cell surface was estimated at 1 pmol/10^8 cells, which represents an approximate number of 7200 molecules/cell.

DISCUSSION

Structural similarity (molecular mimicry) between viral epitopes and self-peptides can lead to the induction of MHC class II-restricted autoaggressive CD4$^+$ T cells (4) as well as MHC class I CD8$^+$ T cell responses (13, 14, 41, 42). Both clinical and experimental evidence continues to accumulate that infectious agents encoding proteins that cross-react with host self-proteins can play a role in molecular mimicry (43, 44).

Data base search for peptides sharing structural homology with a given antigen may be successfully employed to identify potential cross-reactive endogenous ligands (1, 4, 42). Using this strategy, we were able to identify at least five murine self-peptides with predictable high H-2D^b-binding affinity that share with the LCMV NP-(396–404) antigen its main TCR contact residue (Phe at P8). Among these five peptides, three also shared one of the two auxiliary TCR contact residues, either Phe at P1 (protein kinase C-(351–359) and TNFR-(302–310)) or Gln at P4 (lysosomal acid phosphatase-(177–185)). In addition, the TNFR-(302–310) peptide had a third residue in common with LCMV NP-(396–404) (Pro at P3), resulting in a marked functional homology between the viral epitope and the self-peptide (three out of three MHC-binding residues and two out of three TCR contact residues). Yet, we failed to find a murine self-peptide that bore the three TCR contacts of the viral antigen. One may consider that the number of peptides identified by our method was unexpectedly small. However, the small set of self-peptides we found (<10) resembled that of other D^b-restricted (7) or K^b-bound (8) peptides implicated in T cell-positive selection and identified using different approaches. Also, a search for mimicry peptides able to interact with MHC class II-restricted autoreactive T cell clones specific for the myelin basic protein produced a similarly small group (4). These previous results validate our approach, which is further strengthened by the identification of one of these peptides (TNFR-(302–310)) in the material eluted from the surfaces of H-2^b cells.

By which molecular mechanism(s) can the naturally occurring TNFR-(302–310) peptide and the other self-peptides maintain potentially autoreactive CTLs in a functional state? With respect to the NP-specific TCR, TNFR-(302–310) and the other self-peptides identified here behaved as typical altered peptide ligands (45), with implications at both functional and structural levels. At the functional level, despite the presence in their sequences of the main TCR contact and (for some of them) of an additional auxiliary TCR contact, none of the mimicry self-peptides identified here were able to stimulate antiviral CTLs in agonist assays. Nevertheless, they behaved as antagonists, indicating that they still interacted with the TCR and suggesting that their affinity for the NP-specific TCR was relatively low (7). Low affinity recognition of self-MHC promotes thymocyte survival, and in this way, the self-peptides act as low affinity molecular mimics (46). The TCR antagonism we observed may result from impaired TCR triggering. To dissect these TCR-triggering mechanisms further would require exploration of the self-peptides' ability to induce, or not, events such as TCR internalization, TCR dimerization, and phosphorylation of the kinases involved in signal transduction (47). At the structural level, our results support previous studies showing that degenerate recognition of the TCR is not limited to singly substituted variants of a given antigen, but also applies to peptides of originally unrelated sequences (3, 7, 8, 48, 49). Molecular modeling (Fig. 4) revealed that the backbones of LCMV NP-(396–404) and the self-peptide bound to H-2D^b could adopt superimposable conformations. The side chain of Phe at P8 was oriented similarly in the different peptides, a structural feature essential for preserving the function of this residue as the main TCR contact. In contrast, substitution of the viral residue Gly (with no side chain) at P6 for a bulkier self-residue whose side chain points out of the MHC groove clearly created a structural alteration of the peptide-MHC complex surface susceptible to modify (inhibit) the local interactions between the TCR and the MHC α chains. Indeed, alterations of the peptide structure not directly affecting TCR contacts may influence, locally or at distance, the determinants and/or the antigenic surface of the peptide-MHC complex interacting with the TCR (50–53). Furthermore, the presence of peptide side chains that sterically hinder the TCR interaction with the MHC helices results in lowered TCR affinity (54).

What pathophysiological role can a self-peptide like TNFR-(302–310) play? The identification of TNFR-(302–310) as a self-peptide naturally presented by MHC class I molecules lends support for its biological relevance. The TNFR-(302–310) peptide originates from the TNFR-I protein, a cell-surface receptor for tumor necrosis factor-α (55). TNFR-I is highly expressed in the thymus, spleen, and liver (56). In accord, we found that TNFR-(302–310) was naturally present on the surfaces of H-2^b spleen cells at 1 pmol/10^8 cells, a level comparable to that of other self-peptides on the surfaces of thymic epithelial cells and implicated in positive selection of CTLs (7). Evidence that TNFR-(302–310) has a role *in vivo* in shaping the peripheral T cell repertoire, as its natural presence on spleens cells might suggest, would require further experimentation.

In conclusion, the work presented here addresses some fundamental issues regarding the relationship between self- and foreign antigenic peptides in the immune response. In particular, the central point made is that self-peptides such as TNFR-(302–310) and others identified in this study can allow antiviral, potentially autoreactive T cells to keep their cytolytic function in the absence of viral antigen over a period of months. Dissecting the mechanisms by which potentially autoreactive CD8$^+$ T cells are functionally maintained or become activated should provide not only a better fundamental knowledge of pathological autoimmunity, but also new therapeutic concepts for combating it (57). In this study, we focused on MHC class I

self-peptides and hypothesized on their possible role in these mechanisms. Because of the potential importance of these self-peptides in clinical disease, the findings presented here may have important consequences, particularly in terms of therapeutic application, by helping to design peptidic or (better) non-peptidic molecular mimics to target and/or inhibit potentially autoreactive T cells.

Acknowledgments—We thank Honoré Mazarguil for peptide synthesis, Bernard Masri for preparation of peptide extracts, and Monique Erard for molecular modeling.

REFERENCES

1. Oldstone, M. B. A. (1987) *Cell* **50,** 819–820
2. Evavold, B. D., Sloan-Lancaster, J., Wilson, K. J., Rothbard, J. B., and Allen, P. M. (1995) *Immunity* **2,** 655–663
3. Hemmer, B., Vergelli, M., Gran, B., Ling, N., Conlon, P., Pinilla, C., Houghten, R., McFarland, H. F., and Martin, R. (1998) *J. Immunol.* **160,** 3631–3636
4. Wucherpfennig, K. W., and Strominger, J. L. (1995) *Cell* **80,** 695–705
5. Jameson, S. C., and Bevan, M. J. (1995) *Immunity* **2,** 1–11
6. Kersh, G. J., and Allen, P. M. (1996) *Nature* **380,** 495–498
7. Hu, Q., Bazemore Walker, C. R., Girao, C., Opferman, J. T., Sun, J., Shabanowitz, J., Hunt, D. F., and Ashton-Rickardt, P. G. (1997) *Immunity* **7,** 221–231
8. Hogquist, K. A., Tomlinson, A. J., Kieper, W. C., McGargill, M. A., Hart, M. C., Naylor, S., and Jameson, S. C. (1997) *Immunity* **6,** 389–399
9. Sloan-Lancaster, J., Evavold, B. D., and Allen, P. M. (1993) *Nature* **363,** 156–159
10. Klenerman, P., Rowland-Jones, S., McAdam, S., Edwards, J., Daenke, S., Lalloo, D., Koppe, B., Rosenberg, W., Boyd, D., Edwards, A., Giangrande, P., Phillips, R. E., and McMichael, A. J. (1994) *Nature* **369,** 403–407
11. Bertoletti, A., Sette, A., Chisari, F. V., Penna, A., Levrero, M., De Carli, M., Fiaccadori, F., and Ferrari, C. (1994) *Nature* **369,** 407–410
12. di Marzo Veronese, F., Arnott, D., Barnaba, V., Loftus, D. J., Sakaguchi, K., Thompson, C. B., Salemi, S., Mastroianni, C., Sette, A., Shabanowitz, J., Hunt, D. F., and Appella, E. (1996) *J. Exp. Med.* **183,** 2509–2516
13. Misko, I. S., Cross, S. M., Khanna, R., Elliott, S. L., Schmidt, C., Pye, S. J., and Silins, S. L. (1999) *Proc. Natl. Acad. Sci. U. S. A.* **96,** 2279–2284
14. Vizler, C., Bercovici, N., Cornet, A., Cambouris, C., and Liblau, R. S. (1999) *Immunol. Rev.* **169,** 81–92
15. Gairin, J. E., Mazarguil, H., Hudrisier, D., and Oldstone, M. B. A. (1995) *J. Virol.* **69,** 2297–2305
16. Schulz, M., Aichele, P., Wollenweider, M., Bobe, F. W., Cardinaux, F., Hengartner, H., and Zinkernagel, R. M. (1989) *Eur. J. Immunol.* **19,** 1657–1667
17. Murali-Krishna, K., Altman, J. D., Suresh, M., Sourdive, D., Zajac, A., and Ahmed, R. (1998) *Adv. Exp. Med. Biol.* **452,** 123–142
18. Murali-Krishna, K., Lau, L. L., Sambhara, S., Lemonnier, F., Altman, J., and Ahmed, R. (1999) *Science* **286,** 1377–1381
19. Gallimore, A., Glithero, A., Godkin, A., Tissot, A. C., Pluckthun, A., Elliott, T., Hengartner, H., and Zinkernagel, R. (1998) *J. Exp. Med.* **187,** 1383–1393
20. Sourdive, D. J., Murali-Krishna, K., Altman, J. D., Zajac, A. J., Whitmire, J. K., Pannetier, C., Kourilsky, P., Evavold, B., Sette, A., and Ahmed, R. (1998) *J. Exp. Med.* **188,** 71–82
21. Ohashi, P., Oehen, S., Buerki, K., Pircher, H., Ohashi, C., Odermatt, B., Malissen, B., Zinkernagel, R. M., and Hengartner, H. (1991) *Cell* **65,** 305–317
22. Oldstone, M. B. A., Neremberg, M., Southern, P., Price, J., and Lewicki, H. (1991) *Cell* **65,** 319–331
23. Wong, F. S., Karttunen, J., Dumont, C., Wen, L., Visintin, I., Pilip, I. M., Shastri, N., Pamer, E. G., and Janeway, C. A. (1999) *Nat. Med.* **5,** 1026–1031
24. von Herrath, M. G., Dockter, J., and Oldstone, M. B. A. (1994) *Immunity* **1,** 231–242
25. Kagi, D., Odermatt, B., Ohasi, P. S., Zinkernagel, R. M., and Hengartner, H. (1996) *J. Exp. Med.* **183,** 2143–2152
26. Alexander, J., Payne, J. A., Murray, R., Frelinger, J. A., and Cresswell, P. (1989) *Immunogenetics* **29,** 380–388
27. Lewicki, H., Tishon, A., Borrow, P., Evans, C., Gairin, J. E., Hahn, K. M., Jewell, D. A., Wilson, I. A., and Oldstone, M. B. A. (1995) *Virology* **210,** 29–40
28. Hudrisier, D., Mazarguil, H., Oldstone, M. B. A., and Gairin, J. E. (1995) *Mol. Immunol.* **32,** 895–907
29. Falk, K., Rotzschke, O., Stevanovic, S., Jung, G., and Rammensee, H. G. (1991) *Nature* **351,** 290–296
30. Sigal, L. J., Goebel, P., and Wylie, D. E. (1995) *Mol. Immunol.* **32,** 623–632
31. Hudrisier, D., Mazarguil, H., Laval, F., Oldstone, M. B. A., and Gairin, J. E. (1996) *J. Biol. Chem.* **271,** 17829–17836
32. Storkus, W. J., Zeh, H. J., III, Salter, R. D., and Lotze, M. T. (1993) *J. Immunother.* **14,** 94–103
33. Young, A. C. M., Zhang, W. G., Sacchettini, J. C., and Nathenson, S. G. (1994) *Cell* **76,** 39–50
34. Gairin, J. E., and Oldstone, M. B. A. (1993) *J. Virol.* **67,** 2903–2907
35. Byrne, J. A., and Oldstone, M. B. A. (1984) *J. Virol.* **51,** 682–686
36. Jameson, S. C., Carbone, F. R., and Bevan, M. J. (1993) *J. Exp. Med.* **177,** 1541–1550
37. Cao, W., Tykodi, S. S., Esser, M. T., Braciale, V. L., and Braciale, T. J. (1995) *Nature* **378,** 295–298
38. Martin, S., Kohler, H., Weltzien, H. U., and Leipner, C. (1996) *J. Immunol.* **157,** 2358–2365
39. Hudrisier, D., Kessler, B., Valitutti, S., Horvath, C., Cerottini, J.-C., and Luescher, I. F. (1998) *J. Immunol.* **161,** 553–562
40. von Herrath, M. G., Guerder, S., Lewicki, H., Flavell, R. A., and Oldstone, M. B. A. (1995) *Immunity* **3,** 727–738
41. Ohteki, T., Hessel, A., Bachmann, M. F., Zakarian, A., Sebzda, E., Tsao, M. S., McKall-Faienza, K., Odermatt, B., and Ohashi, P. S. (1999) *Eur. J. Immunol.* **29,** 2886–2896
42. Kammer, A. R., van der Burg, S. H., Grabsheid, B., Hunziker, I. P., Kwappenberg, K. M., Reichen, J., Melief, C. J., and Cerny, A. (1999) *J. Exp. Med.* **190,** 169–176
43. Oldstone, M. B. A. (1998) *FASEB J.* **12,** 1255–1265
44. Ruiz, P. J., Garren, H., Hirschberg, D. L., Langer-Gould, A. M., Levite, M., Karpuj, M. V., Southwood, S., Sette, A., Conlon, P., and Steinman, L. (1999) *J. Exp. Med.* **189,** 1275–1284
45. Sloan-Lancaster, J., and Allen, P. M. (1996) *Annu. Rev. Immunol.* **14,** 1–27
46. Goldrath, A. W., and Bevan, M. J. (1999) *Nature* **402,** 255–262
47. Bachmann, M. F., and Ohashi, P. S. (1999) *Immunol. Today* **20,** 568–575
48. Ignatowicz, L., Rees, W., Pacholczyk, R., Ignatowicz, H., Kushnir, E., Kappler, J., and Marrack, P. (1997) *Immunity* **7,** 179–186
49. Hemmer, B., Fleckenstein, B., Vergelli, M., Jung, G., McFarland, H., Martin, R., and Wiesmuller, K.-H. (1997) *J. Exp. Med.* **185,** 1651–1659
50. Chen, W. S., Fecondo, J., and McCluskey, J. (1994) *Mol. Immunol.* **31,** 1069–1075
51. Ono, T., DiLorenzo, T. P, Wang, F., Kalergis, A. M., and Nathenson, S. G. (1998) *J. Immunol.* **161,** 5454–5463
52. Speir, J. A., Garcia, K. C., Brunmark, A., Degano, M., Peterson, P. A., Teyton, L., and Wilson, I. A. (1998) *Immunity* **8,** 553–562
53. Ding, Y.-H., Baker, B., Garboczi, D., Biddison, W., and Wiley, D. (1999) *Immunity* **11,** 45–56
54. Manning, T. C., and Kranz, D. M. (1999) *Immunol. Today* **20,** 417–422
55. Bachmaier, K., Pummerer, C., Kozieradzki, I., Pfeffer, K., Mak, T. W., Neu, N., and Penninger, J. M. (1997) *Circulation* **95,** 655–661
56. Lewis, M., Tartaglia, L. A., Lee, A., Bennett, G. L., Rice, G. C., Wong, G. H., Chen, E. Y., and Goeddel, D. V. (1991) *Proc. Natl. Acad. Sci. U. S. A.* **88,** 2830–2834
57. Green, E. A., and Flavell, R. A. (1999) *Curr. Opin. Immunol.* **11,** 663–669